



RECOMMENDATIONS FOR ENHANCEMENT OF IRRADIANCE QC METHODS

Ref.: D4.4_V1.0

Date: 10/12/2021

Euro-Argo Research Infrastructure Sustainability and
Enhancement Project (EA RISE Project) - 824131

This project has received funding from the European Union's Horizon 2020
research and innovation programme under grant agreement no 824131.
Call INFRADEV-03-2018-2019: Individual support to ESFRI
and other world-class research infrastructures





Disclaimer:

This Deliverable reflects only the author's views and the European Commission is not responsible for any use that may be made of the information contained therein.

Document Reference

Project	Euro-Argo RISE - 824131
Deliverable number	D4.4
Deliverable title	Recommendations for enhancement of Irradiance QC Methods
Description	
Work Package number	WP4
Work Package title	Extension to biogeochemical parameters
Lead Institute	Sorbonne Université
Lead authors	Quentin Jutard
Contributors	Emanuele Organelli, Fabrizio D'Ortenzio, Hervé Claustre, Catherine Schmechtig
Submission date	2021/12/10
Due date	[M36] - 2021/12/31
Comments	
Accepted by	Fabrizio D'Ortenzio

Document History

Version	Issue Date	Author	Comments
Ver. 1.0	2021/12/10	Quentin Jutard	

EXECUTIVE SUMMARY

This document presents an overview of the work that has been conducted on the quality control (QC) of irradiance in the context of the Euro-Argo RISE project. Most of it relates to the delayed mode quality control (DMQC) for which two processes with different scopes were developed. One of these processes was retained and implemented operationally, it allows for the correction of potential issues with the dark values of irradiance instruments.

The accepted process was attempted on all no longer profiling coriolis floats equipped with radiometers, it was applicable in 76% of cases. Around half of the radiometric Argo profiles in coriolis have been passed in delayed mode with this process.

TABLE OF CONTENTS

Introduction	7
1 Real-Time QC	8
2 Delayed mode QC - R&D	9
2.1 Organelli’s method: profile shape screening	10
2.1.1 Rationale	10
2.1.2 Implementation	10
2.1.3 Dataset tested	13
2.1.4 Results	13
2.2 DARK value correction	14
2.2.1 Rationale	14
2.2.2 Implementation	14
2.2.2.1 <i>Sensor temperature reconstruction</i>	14
2.2.2.2 <i>DARK value correction</i>	15
2.2.2.3 <i>Alternative correction methods</i>	20
2.2.3 Dataset tested	20
2.2.4 Results	21
3 Delayed Mode QC - Operational	25
3.1 Recommended process moving forward	25
3.1.1 Gather ancillary data	25
3.1.2 General process	25
3.1.3 Visual QC	26
3.1.4 RADM operations	28
3.2 Process to correct past data	28
3.3 Additional information in DM files	28
3.3.1 QC flags	29
3.3.2 Errors	29
3.3.3 Metadata	29
4 Database improvements and conclusion	30



Appendix : RADM tutorial	32
References	35

Introduction

Part of the existing BGC-Argo array is able to acquire photosynthetically available radiation (PAR) and downward irradiance at different wavelengths. The rationale to have radiometric observations on profiling floats is twofold. First, irradiance and other radiometric quantities are key environmental parameters for addressing the variability of biological processes and for defining the bio-optical status of open-ocean upper water masses. Second, radiometric measurements are also a source of data for validating ocean color radiometry measurements and biogeochemical products from space (Organelli et al., 2016, Claustre et al., 2010).

In November 2021, there were 41908 radiometric profiles, 3721 since the beginning of 2021 with 61 active sensors in October 2021.

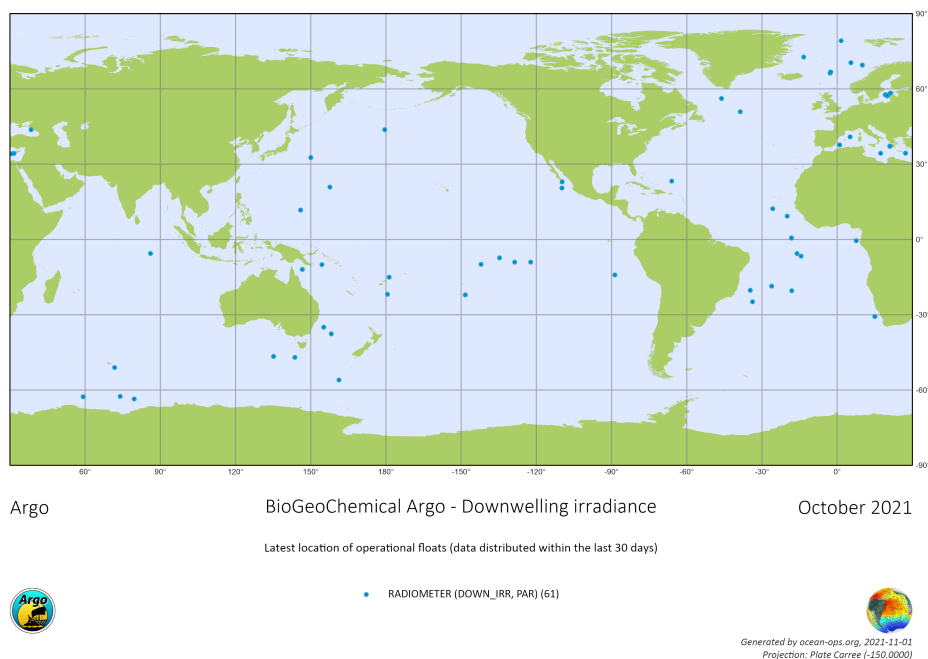


Figure 1: Active floats with radiometers in October 2021 (<https://www.jcommops.org/board>).

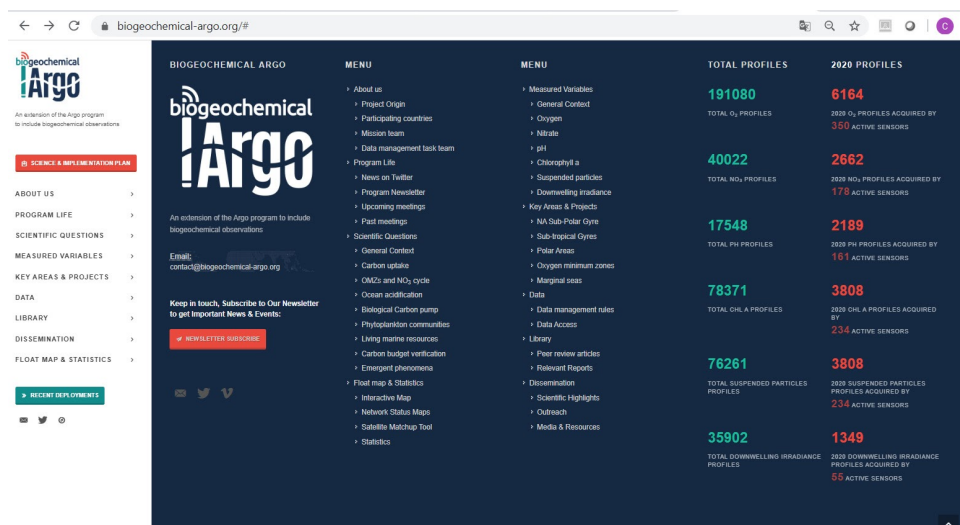


Figure 2: Total downwelling irradiances profiles in Argo and profiles of irradiance acquired since the beginning of 2020 (<https://biogeochemical-argo.org/measured-variables-downwelling-irradiance.php>)

1 Real-Time QC

A first version of the Real Time (RT) Quality Control (QC) procedure was presented at the ADMT16, in Bermuda 2015. This version was not adopted because it was too limiting as it was mainly designed for bio-optical studies (*i.e.* light diffusion, ocean color validation). Subsequently, after studying about eight years of operational radiometric data, no specific sensor issue was identified that could be correctable in RT.

Consequently only a simplified RT QC procedure was implemented (Poteau et al., 2019), that was presented and adopted at the ADMT20 in Villefranche sur mer in October 2019 and further implemented to the Coriolis processing chain. It was fully applied on all radiometric profiles in February 2020.

All of the Coriolis and BODC floats equipped with radiometers are by now processed by the Coriolis processing chain and then are also quality controlled in Real Time.

The simplified RTQC procedure is based on a single test GLOBAL RANGE which applies a range filter on each observed value for DOWN_IRRADIANCE_{xxx} (where xxx is the wavelength in nm) and DOWNWELLING_PAR vertical profiles. The test's threshold values are specific to each variable and represent the maximum value that is expected on the ocean surface under clear sky, regardless of the time of the year. They have been derived from the theoretical model by Gregg and Carder (1990), although they have been finally multiplied by 2 to account for additional effects on radiometric values such as wave focusing. The values used for the GLOBAL RANGE test are listed in Table 1. If an observed data value fails this test, it should be flagged as bad data ("4").

The GLOBAL RANGE test has been applied on the GDAC database on July 25, 2019. Statistics on the results of this test are shown on table 2. Overall, the GLOBAL RANGE test flagged values from 25 of the 186 WMO floats with PARAM DOWN_IRRADIANCE_{xxx} and/or DOWNWELLING_PAR (Table 2).

PARAMETER	Min	Max
DOWN_IRRADIANCE380	-1	1.7
DOWN_IRRADIANCE412	-1	2.9
DOWN_IRRADIANCE443	-1	3.2
DOWN_IRRADIANCE490	-1	3.4
DOWNWELLING_PAR	-1	4672

Table 1: Range values of the global range test. DOWN_IRRADIANCExxx is in $W m^{-2} nm^{-1}$, DOWNWELLING_PAR is in $\mu molQuanta m^{-2} s^{-1}$.

PARAMETER	DOWN_IRRA- DIANCE380	DOWN_IRRA- DIANCE412	DOWN_IRRA- DIANCE443	DOWN_IRRA- DIANCE490	DOWN- WELLING_PAR
NB VALUE	8892018	9107436	215418	9107436	9107436
NB VALUE QC=1	8889437	9049007	215418	9060517	9025518
% QC=4	0.03%	0.64%	0.00%	0.52%	0.90%
MIN before QC	-4.6196	-6.7893	-0.0021	-17228304	-10812
MAX before QC	4.3118	6.3650	2.7591	298833215488	4236
MIN after QC	-0.9541	-0.8021	-0.0021	-0.9989	-1.0000
MAX after QC	1.4148	2.6241	2.7591	3.1826	4236

Table 2: The impact of the global test range on the global radiometric database on July 25, 2019. MIN/MAX values are in $W m^{-2} nm^{-1}$ for DOWN_IRRADIANCExxx and in $\mu molQuanta m^{-2} s^{-1}$ for DOWNWELLING_PAR.

2 Delayed mode QC - R&D

To date, independent data sets of Irradiance or PAR profiles are not available to evaluate the quality of the radiometric float profiles, whether qualitatively or quantitatively. To improve QC, in particular for Delayed Mode (DM) two methods were explored in the framework of Euro-Argo RISE activity.

The first method (Organelli et al. 2016) grades profiles and individual points based on their regularity (evaluated by a polynomial regression) and focuses on the brighter section of profiles. The second method corrects the dark value of profiles on the basis of data measured in the dark, it mostly affects the deeper and darker part of radiometric profiles. In the end, only the latter method was used in operational DM.

2.1 Organelli's method: profile shape screening

A more complete description of the method is available in Organelli et al. (2016). In this section, we will provide a quick overview of the method and its results.

2.1.1 Rationale

A specific data processing was developed to generate BGC-Argo radiometry data which match criteria of quality for Bio-optical applications (Organelli et al., 2016, 2017). In particular, the Organelli et al. (2016) algorithms reconstructed partially the observed profiles, to specifically remove some environmental perturbations of radiative underwater field, which could prevent the application of bio-optical analysis. This approach was considered not matching the BGC-Argo RT QC philosophy, which considers as good all the data not impacted by sensor artefacts.

In a DM QC framework, however, the Organelli et al. (2016) approach could be pertinent: the profiles passing the highly limiting tests of Organelli et al. (2016) could be considered as having passed the visual QC. This would allow the DM operator to focus more attention on the profiles that require it during the visual QC.

Organelli et al. (2016) approach provides a method to identify the modifications of irradiance and PAR profiles generated by:

- Cloud cover during the acquisition phase
- Wave focusing
- Values measured in the dark (deeper part of profiles) which have a low signal to noise ratio

2.1.2 Implementation

The Organelli et al. (2016) method provides a first classification of a radiometric profile (The routines will be available on github), on the basis of a polynomial law fit in log-scale and on the resulting r^2 . A radiometric profile is categorized in one of the following groups:

- Type 1 (good) profiles are smooth with sporadic clouds (figure 3.a)
- Type 2 (probably good) profiles are noisier (figure 3.b)
- Type 3 (suspect) are very noisy profiles or night profiles (figure 3.d)

The r^2 thresholds are parameter dependent and the values for each parameter are shown on table 3. Figure 3 shows a PAR profile of each type. This method also allows to affect a QC on each level of a profile, on figure 4 we show 2 profile examples where the levels flagged "3" ("probably bad") have been removed.

In the framework of the DM QC for irradiance, the automatic classification in type 1 could be useful to assist the visual QC of profiles, on figure 7 we provide a suggestion for how it could be done for the 490nm channel. The classification could allow the operator to only visually check the profiles that are of type 3 or that have a high number of outliers (with flag "3"). Alternatively, if they do not want to completely skip over profiles that were classified as good, they can visually validate them separately and at greater speed. This would still allow them to spend more time looking at profiles that require a more attentive visual QC.

Channel	Type 3	Type 2	Type 1
$E_d(380)$	$r^2 \leq 0.997$	$0.997 < r^2 \leq 0.999$	$r^2 > 0.999$
$E_d(412)$	$r^2 \leq 0.997$	$0.997 < r^2 \leq 0.998$	$r^2 > 0.998$
$E_d(490)$	$r^2 \leq 0.996$	$0.996 < r^2 \leq 0.998$	$r^2 > 0.998$
PAR	$r^2 \leq 0.996$	$0.996 < r^2 \leq 0.998$	$r^2 > 0.998$

Table 3: r^2 thresholds to discriminates the shapes of the profiles

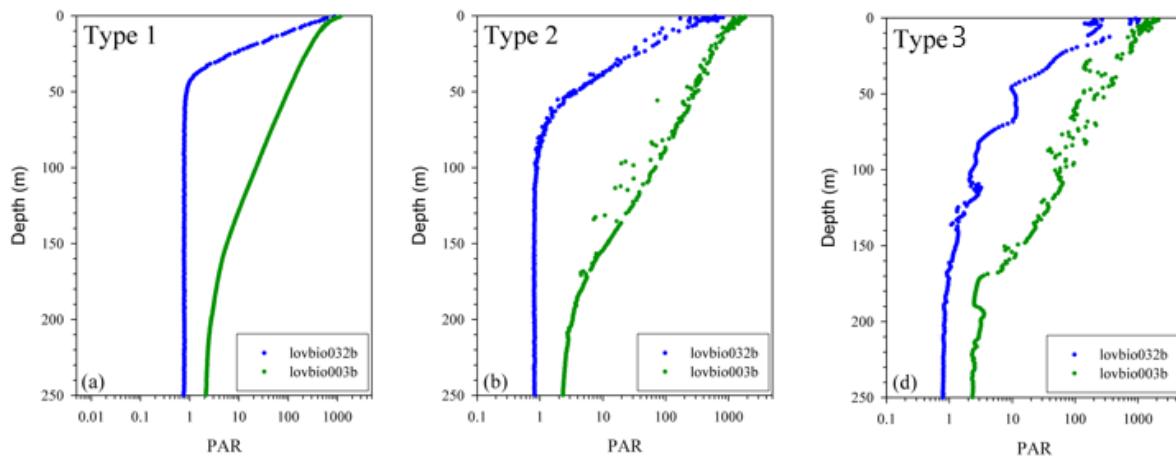


Figure 3: Different type of profiles on float 6901525 (lovbio032b) and 6901437 (lovbio003b).

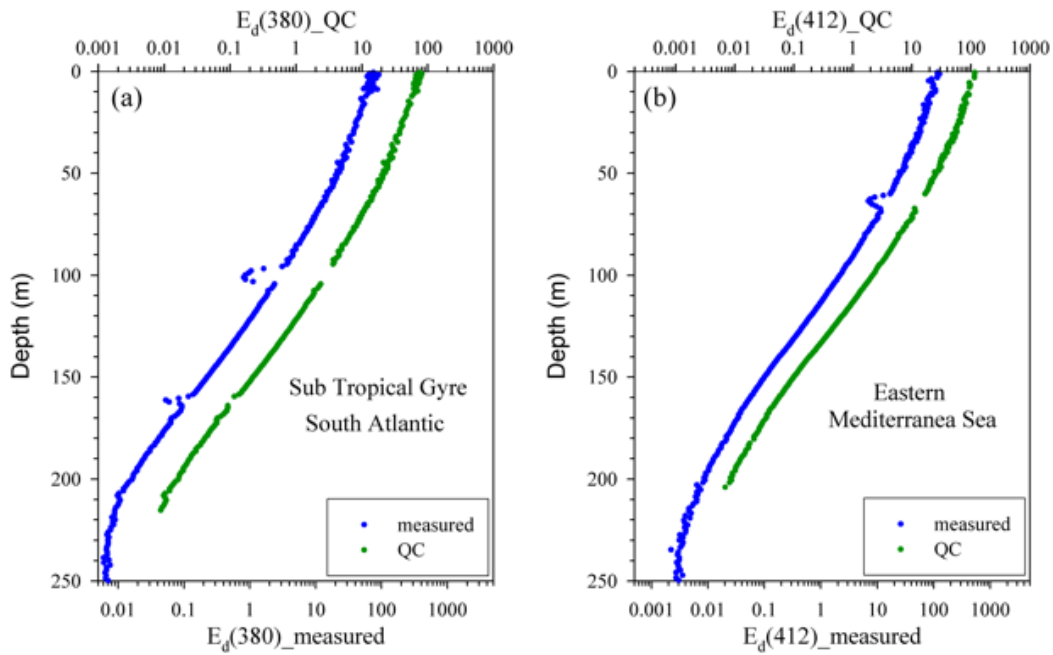


Figure 4: Examples of vertical profiles before ($_{measured}$) and after ($_{QC}$) QC (only points flagged QC=1 and QC=2 are shown on the green profile, QC=3 are removed). Measured and QC profiles are displayed on different x axes only for improved visualization.

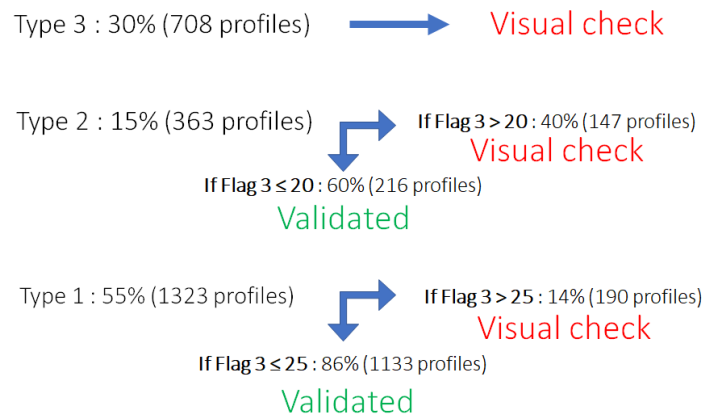


Figure 5: Proposition for the channel at 490nm: how to deal with the profiles classification according to the proportion of points in profile with QC=3.

2.1.3 Dataset tested

To verify the Organelli et al. (2016) approach in the framework of Euro-Argo RISE, seven floats were chosen to be representative of different areas and with different light exposition and environments (see figure 6 for the location of the selected floats). This resulted in a subset of 2394 profiles tested.



Figure 6: Location of the 7 floats tested.

2.1.4 Results

Figure 7 shows, for each radiometric parameter, the proportion of tested profiles that were classified 1, 2, and 3 by the Organelli et al. (2016) method. Most of the profiles are classified as type 1. Overall, the approach of Organelli et al. (2016) provides an efficient method to drastically reduce the number of profiles that would require a final validation by visual inspection. All the Type 1 profiles could be considered automatically “good” whereas the other will require an expert validation.

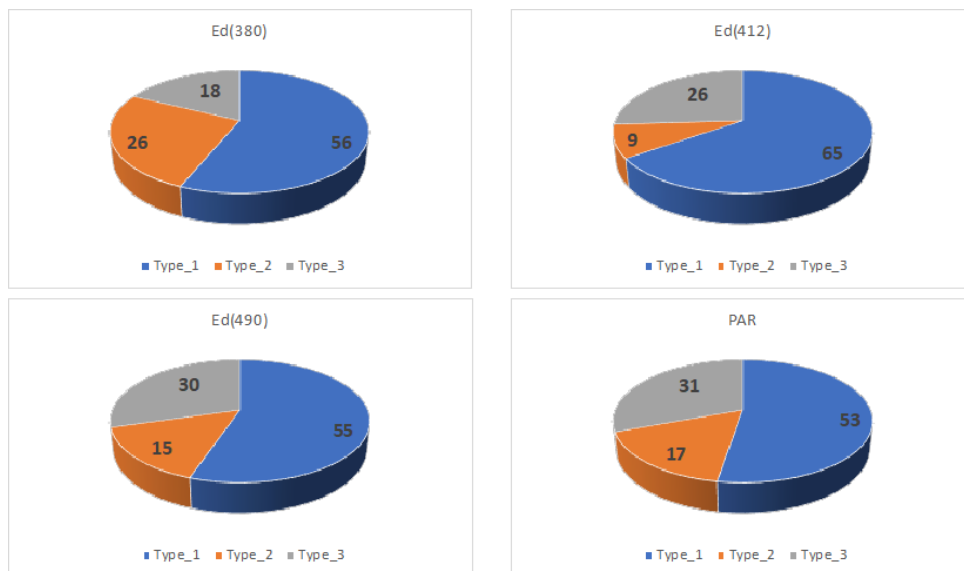


Figure 7: Proportion of each type in percent of the 2394 classified profiles.

2.2 DARK value correction

2.2.1 Rationale

The DARK value of a radiometry sensor is the value that it returns when exposed to no light. The DARK value is a calibration parameter and it is removed from the raw measured data to impose a zero value corresponding to a real zero irradiance. Previous analysis on data obtained under dark conditions demonstrated that the DARK value of radiometers is not temporally constant, this effect will be referred to as aging. Additionally, the DARK value is affected by the instrument's temperature.

There exist conditions under which radiometers embarked on Argo floats have measured radiometry in the dark, namely:

- profiles measured at night.
- measurements obtained during float drift, *i.e.* at 1000 dbar.
- measurements obtained in the deepest part of profiles acquired during the day.

Any non 0 signal measured in the dark corresponds to the variability of the dark value. Drift data have the advantage of covering a large time range with low temperature variability, which allows us to isolate the dark's time dependence. On the other hand, night profile data can cover a temperature range that is comparable to the range that is explored in day profiles, after correcting for the dark's aging they are well suited to estimate the dark's temperature dependence. Data measured in the deep part of day profiles are not as reliably measured in dark conditions but they have the advantage of being available for all floats, they can be used for alternative methods that do not rely on drift data or night profiles (ancillary data).

In the framework of Euro-Argo RISE, methods to realize these corrections have been developed, an overview of the methods is provided here, the details of the process can be found in Jutard et al. (2021).

2.2.2 Implementation

2.2.2.1 Sensor temperature reconstruction

Evidence of temperature effects on the dark value of radiometers had already been provided at ADMT-19 by Xiaogang Xing and Nathan Briggs. They also highlighted that the temperature of the instrument (that affects the dark value) is not equal to the water temperature that is measured at the same depth by the CTD. There is a lag because of the thermal inertia of the instrument.

In the framework of Euro-Argo RISE, specific laboratory experiments were conducted to estimate a literal formulation of this lag; the radiometer's receivers were covered with black tape and the instruments were suddenly moved from a 5°C thermostat to a 30°C thermostat (Jutard et al. 2021). The values returned by the radiometer under these conditions indicate the rate at which heat penetrates the instrument (figure 8).

From the laboratory experiments, a relationship between sensor temperature T_s and water temperature T_w was derived:

$$\frac{1}{k} \frac{dT_s}{dt}(t) = T_w(t - \Delta t) - T_s(t)$$

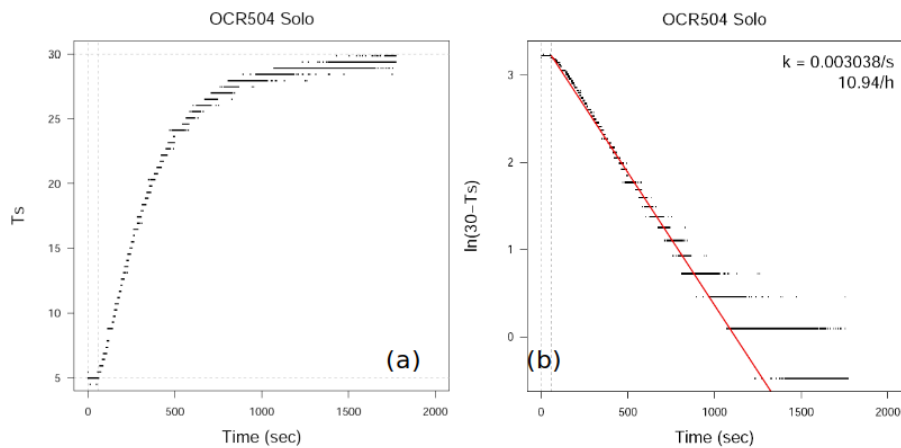


Figure 8: Example internal temperature (T) response to an abrupt change in external temperature. Data are from OCR504 s/n 00021, equilibrated at 5°C and immersed in 30°C water: (a) x-axes show time since immersion and y-axes show T ; (b) the natural logarithm of the difference between ambient and internal temperature. Red line in panel (b) shows regression used to estimate heat transfer coefficient k , shown in text within the figure. Source: Jutard et al. 2021.

Where t is time and k and Δt are empirical coefficients obtained from the same experiments. These coefficients are a function of the physical properties of the instrument and are different from one instrument model to another. Presently, two different instrument models equipped the BGC-Argo fleets: both are OCR-504 radiometers (Sea-Bird Scientific), although the materials used differed. In most cases, instruments are encased in PEEK (Poly-Ether-Ether-Ketone) whereas some early instruments were encased in aluminum. Values for k and Δt for both cases are provided in Jutard et al. 2021.

Knowing the relationship between T_s and T_w it is possible to reconstruct the radiometric sensor temperature in Argo profiles from the CTD temperature.

2.2.2.2 DARK value correction

The method to correct the sensor's dark dependence on temperature and aging is composed of 2 steps:

1. Aging correction: Correct the sensor's dark aging with the help of the drift data (measured in between profiles at 1000 dbar).
2. Temperature effects correction : Correct the sensor's dark temperature dependence with the help of the night profiles (which have been corrected for aging from the first step).

The corrections can be computed automatically by the specially developed RADM code base (https://github.com/qjutard/radiometry_QC). This code automatically computes the correction steps and presents the operator with figures similar to figures 9, 10, and 11. The operator can then validate the proposed correction or make relevant decisions. The details of the software possibilities and the operator decision tree will be presented in the operational section (see section 3.1.2).

Aging correction

Drift data is used to correct aging because at this depth, no light is present and temperature varies little, this means that the measured signal is directly related to aging. However, the low temperature variations can still have a visible effect on the measured signal, which needs to be accounted for. Figure 9, which shows the Irradiance drift measurements of float 6901584, colored by temperature, is an example of the effect of low temperature variability at 1000 dbar with high impact on the sensor's dark value.

When this low temperature variability is accounted for, the sensor's dark aging can be fitted linearly against time (like PAR, $E_d(380)$, and $E_d(490)$) in figure 10). In practice, this is done with a bi-linear regression of the measured signal over time and temperature. In some cases the operator may find that the dark's aging would be better fitted quadratically against time, this has been included as an option in RADM and has been done for $E_d(412)$ in figure 10. The operator verifies visually with figures 9-10 that the modeled aging is a good representation of the drift data, figure 10 is also plotted over the entire lifespan of the float so that the operator may validate the amount of extrapolation from the drift data that will be necessary for the DM correction.

Please note that we do not mean here that in this case the aging is a quadratic function of time, the quadratic fit is just a model of the observed behaviour. This behaviour may be better described as a broken line, with sensor aging always being linear but changing in direction and/or intensity following a perturbation, but the quadratic fit is more easily applicable and is flexible enough to represent this behaviour.

If the operator is not satisfied with the proposed aging correction, they may decide to attempt the temperature effects correction anyway. This is an option offered in RADM and should especially be considered for floats with a short lifespan.

Temperature effects correction

After correcting night profiles for the sensor's dark aging, we can plot the measured values against the sensor temperature (as reconstructed in section 2.2.2.1), this is done in figure 11. We can then compute the linear regression of the dark value against temperature, the result of which is also shown on figure 11. Similarly to the aging correction, the operator must validate the adequacy of the fit and the quality of the ancillary data, the figure is also plotted with the full range of temperature ever encountered by the sensor so that the operator may judge the amount of extrapolation from night data that will be required for the DM correction.

Finally, the aging correction and the temperature effect correction can be combined and applied to all the profiles. It should be noted that in order to apply the correction to day profiles, the sensor temperature will need to be reconstructed as in section 2.2.2.1.

The RADM software can apply the correction automatically, as well as QC flags, error axes, and metadata (all of which will be detailed in the operational section).

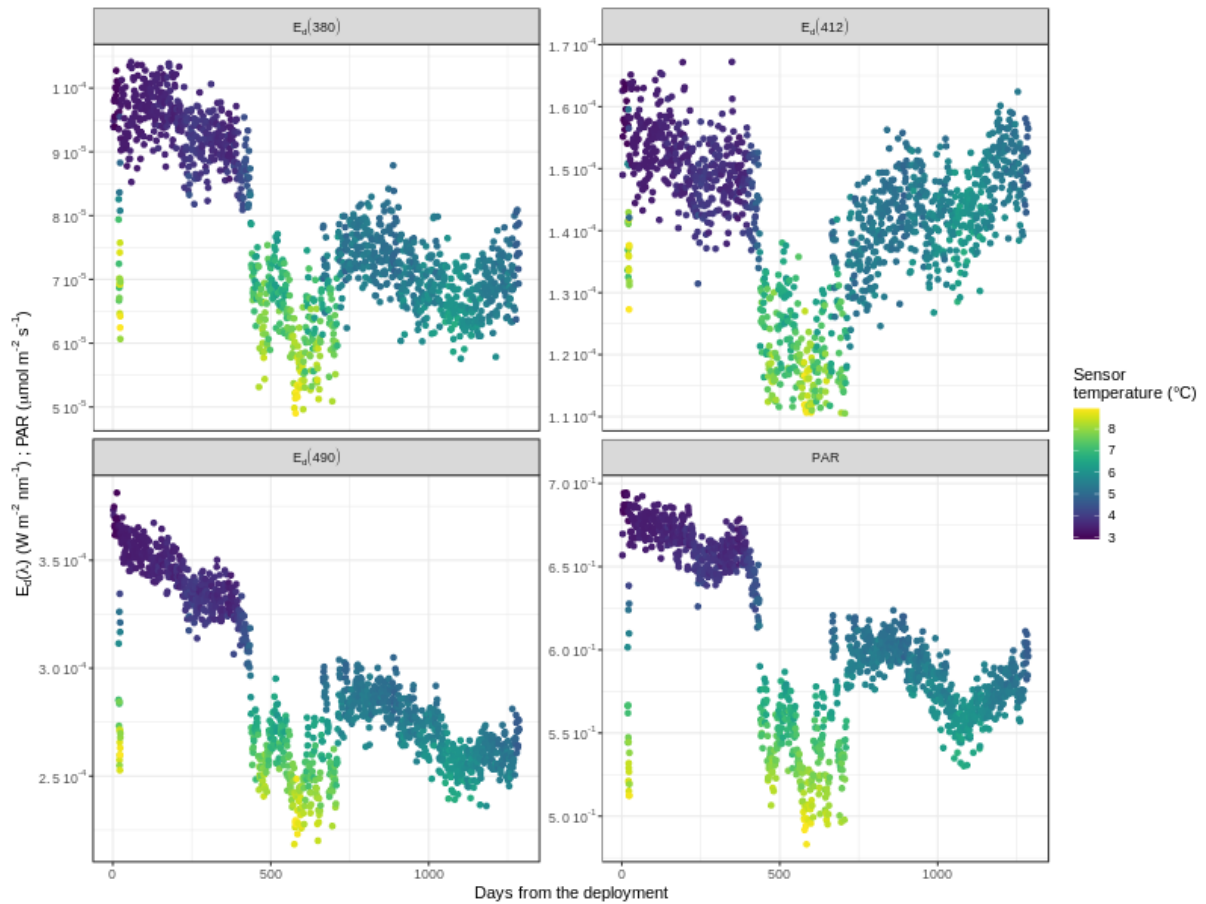


Figure 9: Radiometry drift measurements for $E_d(\lambda)$ and PAR as a function of time and temperature. Example is shown for the float WMO6901584. Source: Jutard et al. 2021.

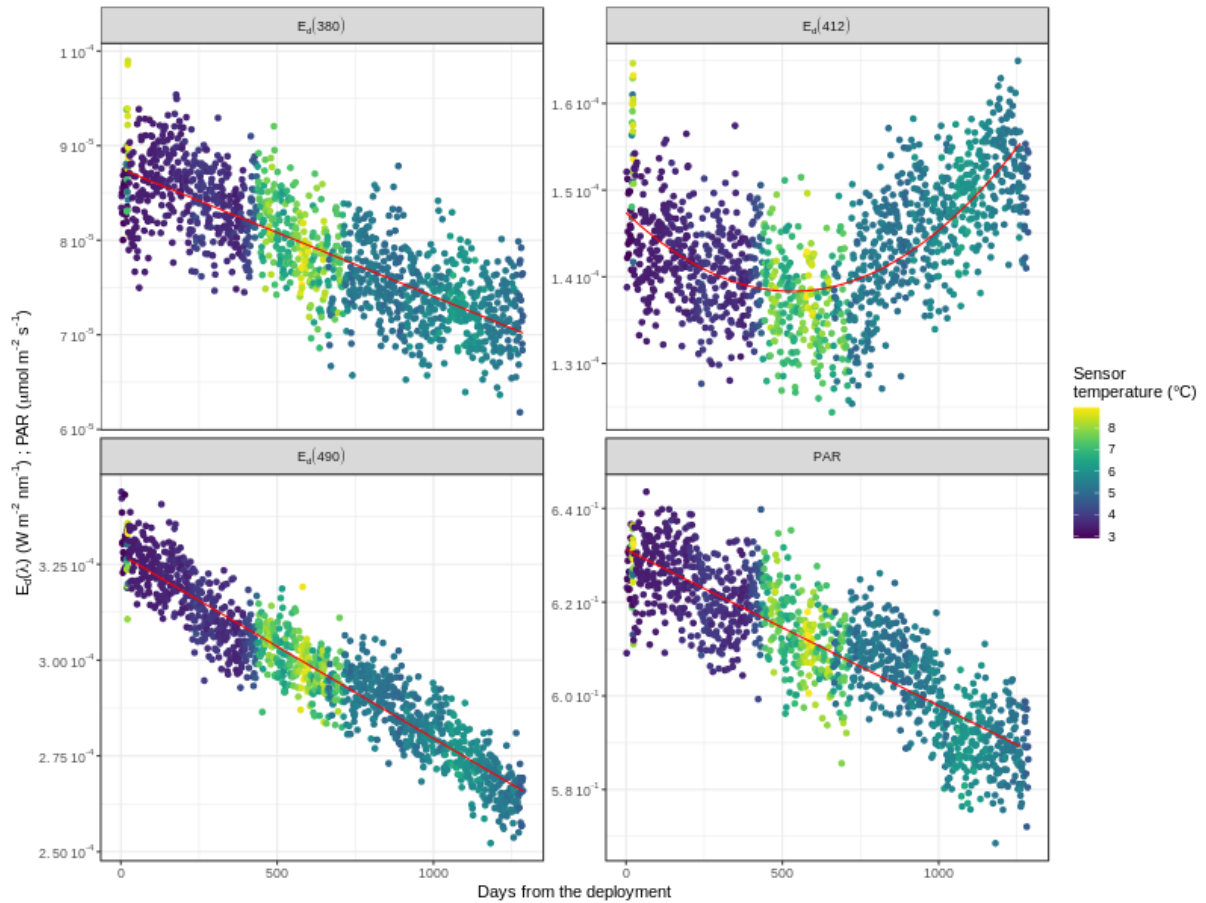


Figure 10: Radiometry drift measurements for $E_d(\lambda)$ and PAR as a function of time after estimation at a reference temperature of 5°C. Solid line is the fit to all points. For this float, the fit is linear for all channels but $E_d(412)$. Example is shown for the float WMO6901584. Source: Jutard et al. 2021.

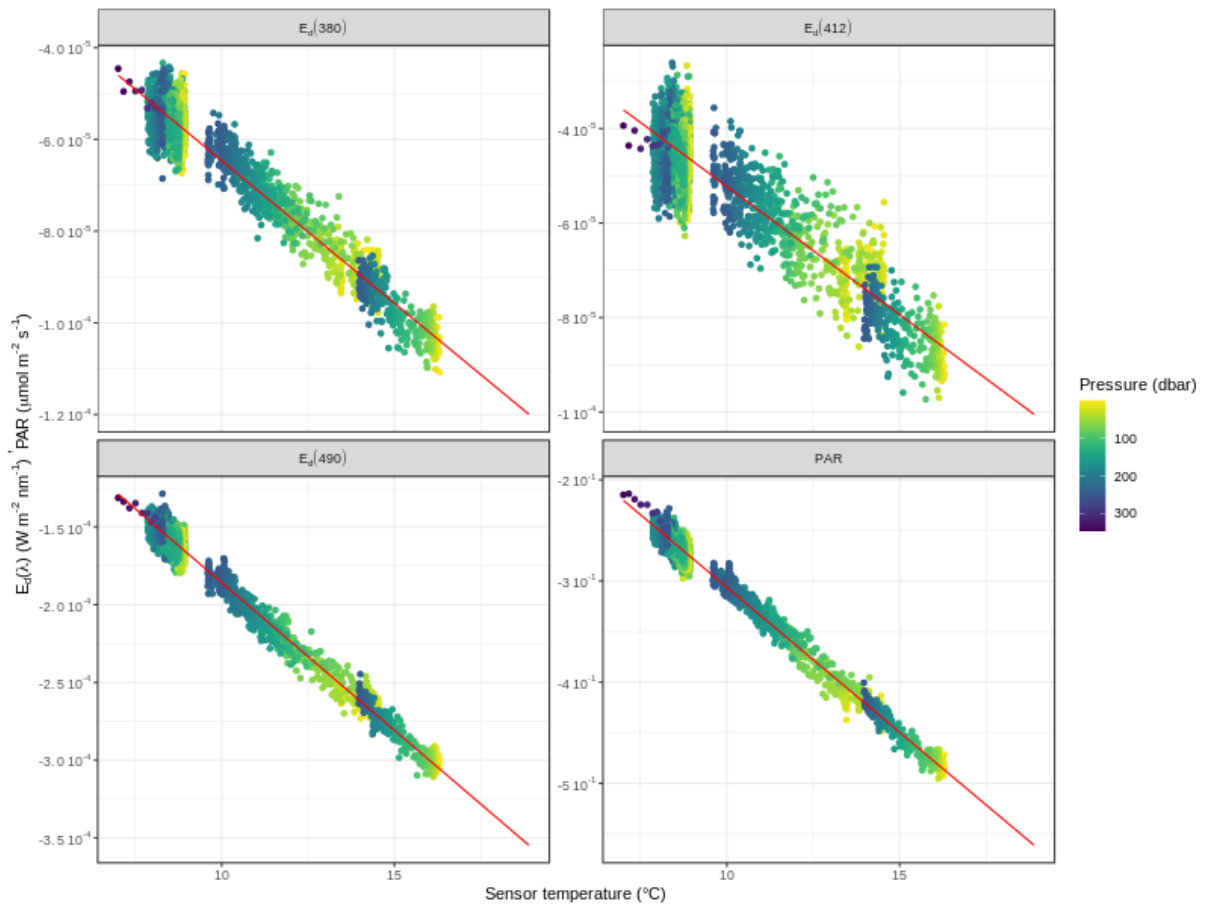


Figure 11: Radiometry night profiles of $E_d(\lambda)$ and PAR as a function of sensor internal temperature T_s . Dots are colored according to pressure. Solid red line is the fit to all points, and is extrapolated to cover the entire range of temperature encountered by the float during the whole lifetime. Prior to computing the linear regression, night profiles have been corrected for any sensor aging. Example is shown for the float WMO6901584. Source: Jutard et al. 2021.

2.2.2.3 Alternative correction methods

The previous methods are applicable only when observations during drift and night profiles are available. This is not always the case, in particular for old floats. To correct the data obtained from these floats, alternative methods for aging and temperature effects are proposed. The proposed methods do not rely on ancillary data. They use observations from the deep part of profiles, which are identified with successive lilliefors tests following Organelli et al. 2016. The working hypothesis is that the deepest part of a radiometric profile is generally measured in the dark. Using this section of deep observation, the methods are similar to the preferred methods detailed in the previous section and include a validation of figures similar to figures 9, 10, and 11 by the DM operator. The details of these alternative methods, as well as an example of a float processed in DM with these methods, are available in the supplementary of Jutard et al. 2021.

However, the working hypothesis (*i.e.* deep data observed in the dark) as well as the methodology to extract the dark values are not automatically verifiable. In these cases, then, the final visual validation of the DM plots (figures 9-11) has to be done with even greater care.

The RADM software will compute these alternative methods by default and present them to the operator alongside the main procedure in plots similar to figures 9, 10, and 11. In some cases where ancillary data (drift or night) are available but sparse or messy, the operator may prefer to apply the alternative correction, this is an option in RADM.

2.2.3 Dataset tested

We considered all of the (at the time) 131 no longer profiling coriolis floats equipped with radiometers. Measurements of radiometric parameters in drift started to be acquired in mid 2014, floats are considered to have a good coverage of drift measurements if they measured at least 80% of their profiles after this date. A night profile is defined as a profile measured when the solar elevation is lower than -5° at the time stored in JULD and the location of the profile. We determined whether the 131 considered floats had acquired any night profiles, and whether they had acquired drift data for at least 80% of their lifetime, this is shown on table 4.

Number of floats with...	...drift acquired for >80% of the float's lifetime	...drift acquired for ≤80% of the float's lifetime	Total
...night profiles	55 (12867)	41 (7582)	96 (20449)
...no night profiles	10 (1035)	25 (2733)	35 (3768)
Total	65 (13902)	66 (10315)	131 (24217)

Table 4: Availability of night profiles and drift measurement in 131 coriolis floats. The number of radiometric profiles on these floats is expressed in parentheses.

Overall, 55 floats meet the criteria required to apply the preferred methods described in Jutard et al. (2021) and section 2.2.2.2, whereas for the remaining 76, only the alternative methodology can be used (section 2.2.2.3). The alternative methodology was in fact developed specifically for this purpose.

2.2.4 Results

Figure 12 shows an example of the results of the proposed DM QC (aging corrected with drift data, temperature effects corrected with night profiles) over real profiles obtained from 4 floats deployed in different oceanic regions.

In logarithmic scale, the figure shows that the corrected profiles monotonically decrease at a greater depth than non corrected profiles. In linear scale we can see the corrected profile decreasing to near 0 within the error bounds (see section 3.3.2). In particular on subfigures 12.e and 12.h the non corrected profiles had an unrealistic step which was a consequence of the temperature gradient, our process allows us to effectively eliminate these steps.

Applicability of the process

We attempted to apply the methods described previously on all 131 floats and recorded whether the correction was applicable with reasonable confidence. The alternative methods that we described in section 2.2.2.3 were also considered, especially in the cases where ancillary data were missing. We noticed that the aging correction was of lesser importance than the temperature effects correction, we accepted that the former could be skipped.

We considered the method to be applicable if we could at least confidently apply a temperature effects correction, be it the main method or the alternative. In table 5 and figure 13 we show the applicability rate of the whole process, separated depending on the availability of ancillary data. We had more success with floats that measured a large number of profiles because they consequently have a lot of available correction data, so we express the applicability rate in terms of the number of corrected/non-corrected profiles (not floats), which is more representative of the data.

Number of profiles corrected from floats with...	...drift acquired for >80% of the float's lifetime	...drift acquired for <=80% of the float's lifetime	Total
...night profiles	12179/12867 (95%)	5414/7582 (71%)	17593/20449 (86%)
...no night profiles	217/1035 (21%)	502/2733 (18%)	719/3768 (19%)
Total	12396/13902 (89%)	5916/10315 (57%)	18312/24217 (76%)

Table 5: Applicability of the DM process depending on the availability of drift measurements and night profiles.

The combined main and alternative methods have had overwhelming applicability (95%) in cases where the ancillary data is available. In cases with night profiles but without drift data we had a more moderate success rate of 71%. In cases without night profiles we had very limited success with a rate of around 20%. The availability of drift data is less important than that of night profiles, this is expected as we considered the aging correction as optional.

Overall we were able to correct the sensor's dark in a large majority of the past profiles (76%). We expect the future success rate to be even higher (around 95%) as floats will be programmed to measure ancillary data, see our recommendations in section 3.1.1.

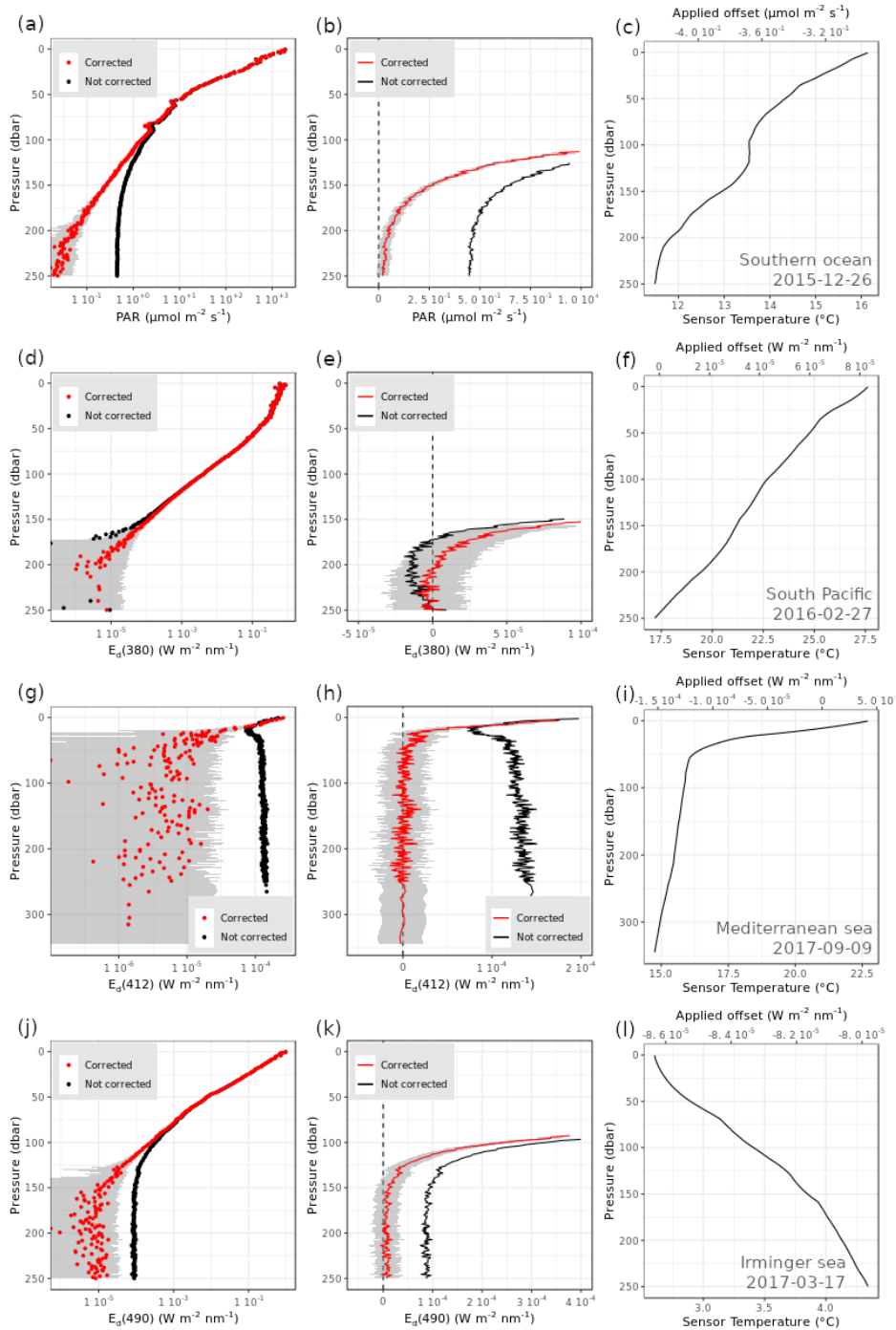


Figure 12: Examples of radiometry profiles before and after DM-QC: Left) profiles are shown in a semi-log scale; Centre) profiles are shown in a linear scale; Right) the reconstructed sensor internal temperature T_{sis} is shown. Examples derive from four BGC-Argo floats deployed in oceanic regions characterized by diverse trophic and optical regimes: (a–c) Southern Ocean; (d–f) South Pacific subtropical gyre; (g–i) Mediterranean Sea; (j–l) North Atlantic subpolar gyre—Irminger Sea. Source: Jutard et al. 2021.

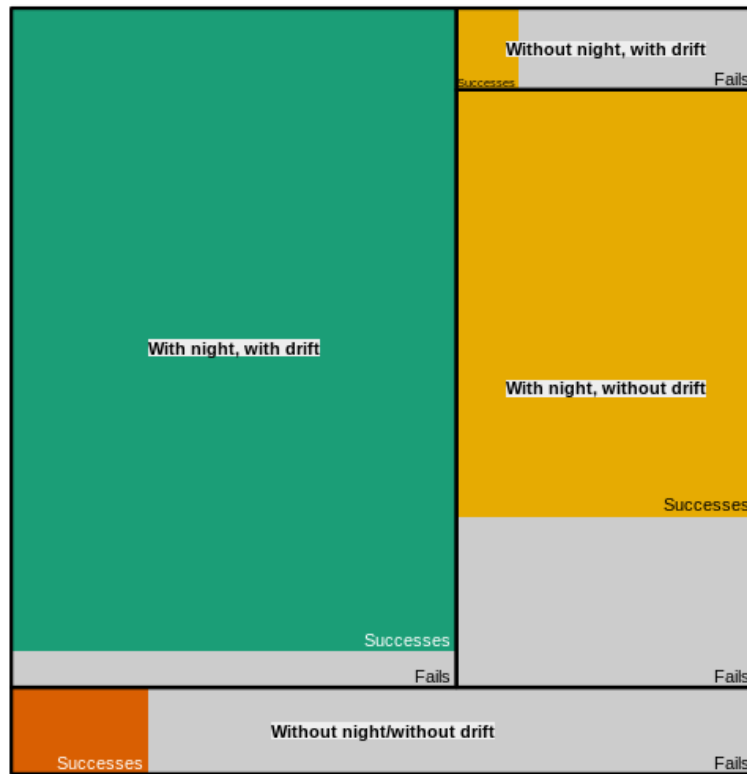


Figure 13: Treemap the applicability of the DM process (including alternative methods). The floats are separated depending on the availability of ancillary data, with green for full availability, yellow for partial availability, and orange for no ancillary data. This figure is based on the numbers from table 5.

Applicability of the main method on floats with good ancillary data

In anticipation of future deployments we wanted to evaluate the success rate of our process when we only use the main methods. We focused this study on the 55 floats with available ancillary data because we expect future deployments to have this data available. In this configuration, we were able to correct all 4 radiometric channels on 46 out of 55 floats, which combined represent 90% of the tested profiles. We show on figure 14 the position of these profiles with colors corresponding to the success of the process. On floats with good ancillary data, the process using only the main methods is almost as successful as the full process, for future deployments we will only recommend using the main methods (see section 3.1.2).

On figure 15, we show the success rate of the process including only the main methods on the 55 floats with good ancillary data, depending on the number of available night profiles. In all cases where 4 or more night profiles were acquired, we were able to provide a correction for the sensor’s dark. Most floats had measured 3 or fewer night profiles, but we were still able to provide a correction for the majority of these floats. The expected lifespan of a BGC-Argo float being 4 years, we can recommend that night profiles be acquired once a year, preferably at a time with a large temperature range in the water column.

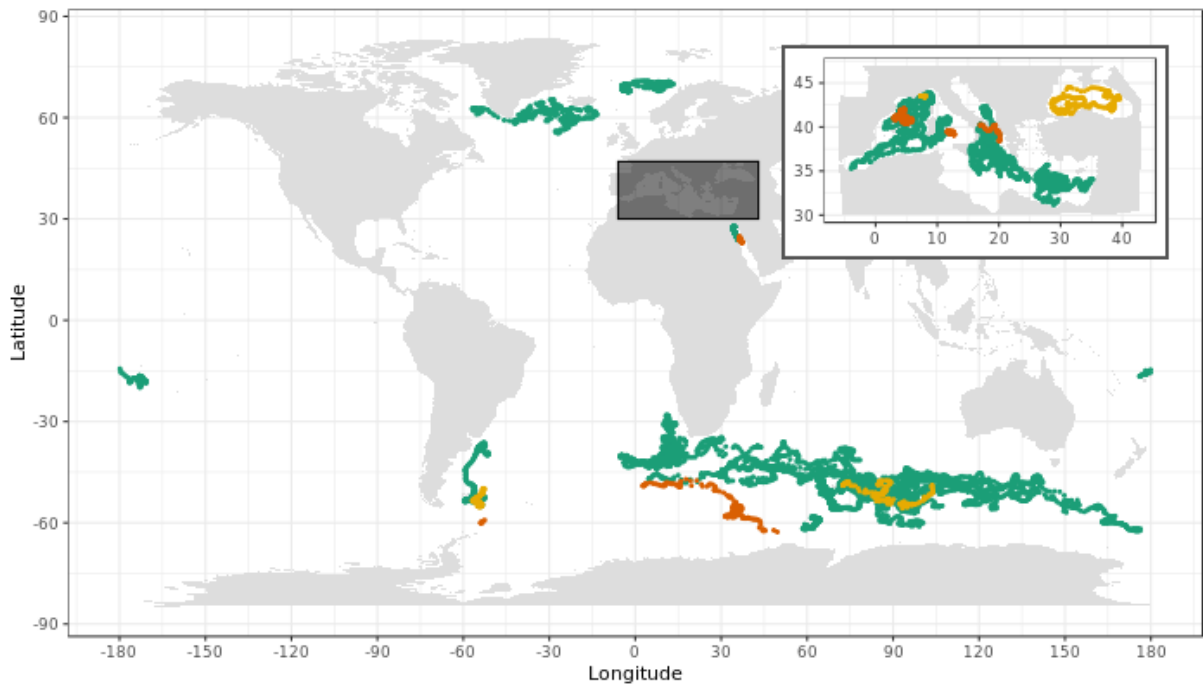


Figure 14: Radiometry profiles acquired by the 55 BGC-Argo floats with ancillary night profiles and drift measurements. Green dots: successfully corrected profiles with the DM-QC procedure; Orange dots: uncorrected profiles; Yellow dots: profiles corrected with alternative methods. Source: Jutard et al. 2021.

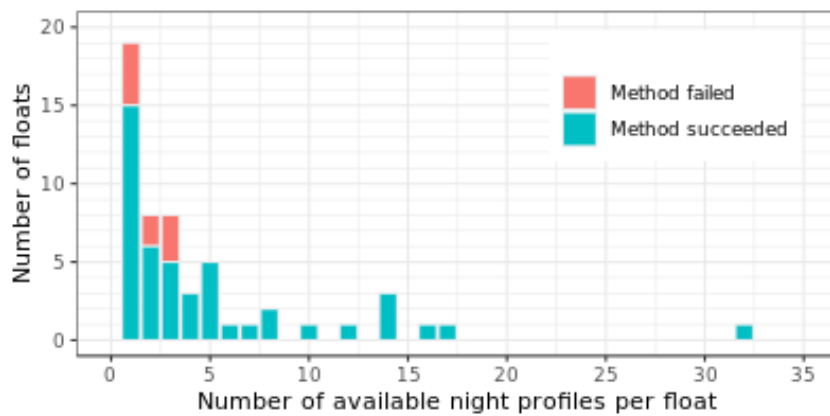


Figure 15: Number of floats with dark measurements successfully corrected (with the main methods) for the four radiometric channels as a function of available night profiles. Source: Jutard et al. 2021.

3 Delayed Mode QC - Operational

Organelli's method focused on eliminating environmental effects that could cause the profiles to depart from the expected monotonic decrease (Shading from clouds, wave focusing). It was decided that the DMQC provided by Argo for radiometry should not filter these effects, therefore the operational DMQC will consist solely of the sensor's dark correction. In future work, it could be interesting to provide a separate dataset that has had dark values corrected (from Jutard et al. 2021) and environmental effects removed (Organelli et al 2016).

3.1 Recommended process moving forward

3.1.1 Gather ancillary data

Our first, and most important, recommendation is to acquire drift data and night profiles to facilitate the DMQC. Drift data acquisition is already programmed in almost all newly deployed floats, but night profiles are still obtained irregularly.

We recommend that floats equipped with radiometers acquire at least one night profile per year, preferably during the season with the largest temperature range in the water column. We recommend that these night profiles be measured from the same depth and with the same frequency as a typical day profile measured by the considered float.

3.1.2 General process

For future float deployments, ancillary data should be available from our recommendations. For this reason we recommend correcting the sensor's dark with the preferred methods described in section 2.2.2.2. These methods have been implemented in the RADM codebase (https://github.com/qjutard/radiometry_QC), which we have used to successfully correct 81 of the 131 no longer profiling coriolis floats equipped with radiometers. RADM can handle all of the DM operations except for the visual QC, for which we recommend Scoop-Argo.

On figure 16 we present a flowchart of the full DM process with numbered steps that will be detailed hereafter. After the visual QC is done with Scoop-Argo (step 1, see section 3.1.3), the first sensor aging estimation is computed with RADM (step 2). This first estimation uses linear fits to the drift data and presents the results to the operator (through plots similar to figures 9 and 10). Then, the operator decides whether the proposed correction is adequate on the basis of the quality of the drift data and the adequacy of the linear fits (step 3). The time axis on these plots is made to cover the full lifetime of the float which allows the operator to also notice if the correction would need to be extrapolated from a relatively narrow range of data. In such a case it is not recommended to accept the correction, this is especially true if the drift data has been fitted quadratically.

If the first linear fit is not satisfying for any of the reasons stated, the operator is provided with the option to use a quadratic fit in time for any number of radiometric channels (steps 4 and 5). This can be used if the operator notices that the sensor's dark aging has changed in direction and/or intensity.

If neither linear nor quadratic fits are satisfying, we recommend to continue without an aging correction as the temperature effects correction is significantly more important (step 6).

As shown on figure 16 the process for the correction of temperature effects is fairly similar. The initial correction is computed and presented to the operator on a plot similar to figure 11 (step 7), the

operator then decides whether to accept it or not on the basis of the quality of the night profile data and the adequacy of the fits (step 8). Similarly to the time axis in the aging correction step, the temperature axis is extended to cover the full range of temperature that the float encountered so that the operator can evaluate the level of extrapolation.

Night profiles may contain some significant signal at shallow depths if moonlight is present or if the profile was measured near dawn or dusk. In such a case, the operator may set a pressure threshold in RADM to cut the shallowest data from night profiles (steps 9 and 10). If no satisfying correction for temperature effects can be found, the operator should abandon the DMQC for this float (step 11).

When the operator validates the temperature correction, RADM will compute the corrected profiles based on the aging/temperature correction and create the corrected netCDF B-files with the adequate appropriate information (step 12, see section 3.3).

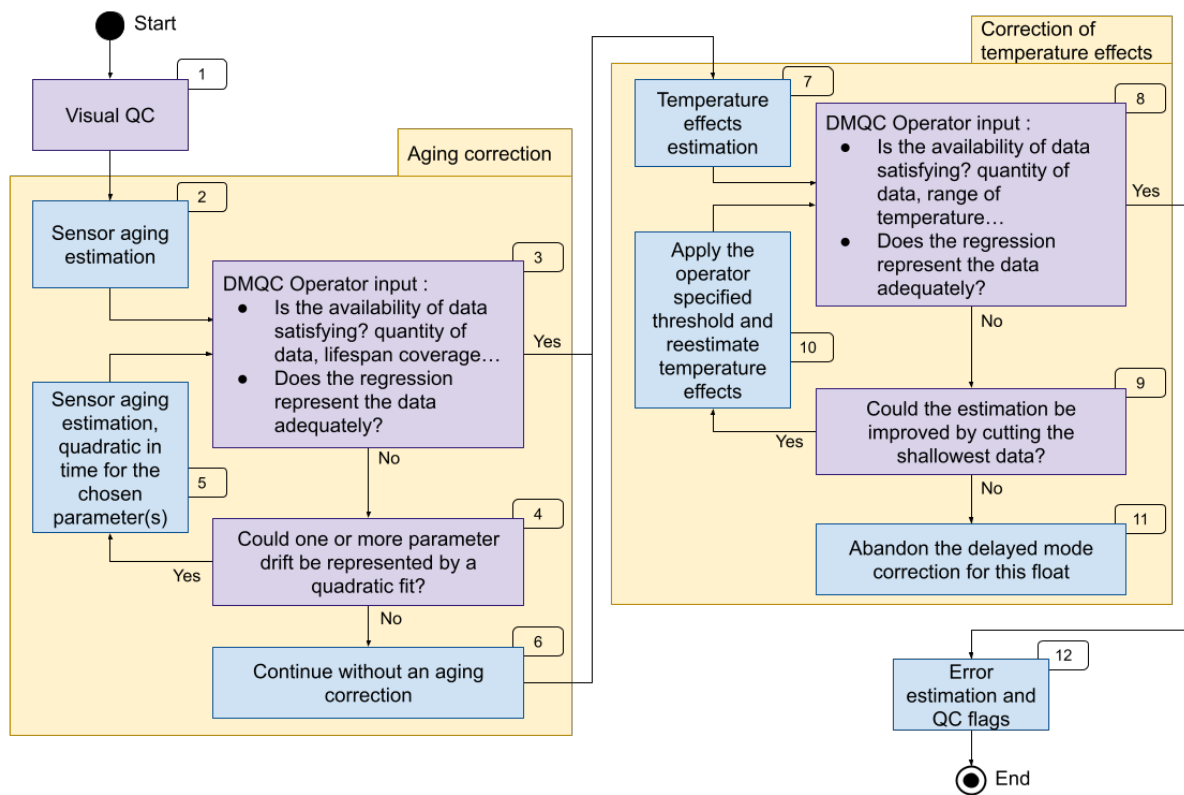


Figure 16: Flowchart of the QC procedure to correct radiometry sensor's dark for aging and temperature dependency. Steps in blue can be handled with RADM (see section 3.1.4), steps in purple require decisions from the operator. Source: Jutard et al. 2021.

3.1.3 Visual QC

The visual QC can be performed with Scoop-Argo (See a screenshot of the visual QC in progress on figure 17), which updates the `PARAMETER_QC` axis (not `PARAMETER_ADJUSTED_QC`). The `PARAMETER_QC` in-

formation is then used to remove “bad” and “probably bad” data (respectively QC flags “4” and “3”) from consideration when computing the DM corrections, it is also the basis of the PARAMETER_ADJUSTED_QC axis that is computed by RADM (see section 3.3.1).

Validate/invalidate the points removed by the RTQC

The RTQC sets the flags to “1” (“good data”) except when the values are outside of the range test where the flags are set to “3” (“probably bad”). In some cases, the value at depth of profiles for one radiometric channel was consistently negative and lower than the lower bound of the range test of the RTQC. In such a case, values at depth are considered unrealistic and flagged by the RTQC (flag “3”). If the DM operator estimates that this data can be corrected by the DMQC, they should overrule the range-test and change the flags from “3” to “1” or “2”. By doing this, the data are taken into consideration for the DMQC operations and subsequently corrected.

Screen all profiles

Then the operator should have a look at all the profiles and mark any data that they find dubious as either “3” or “4” (“probably bad” or “bad”), they may also mark some data as “2” (“probably good”) if they want to mark it as slightly dubious but not enough to be excluded. The distinction between “1”/“2” and “3”/“4” data is important as the data marked “3” or “4” will be excluded from the DM operations. On the other hand, the finer distinction between “1” and “2” and between “3” and “4” is left to the operator.

The most commonly occurring issue that should be removed during the visual QC is shown on figure 17. There often is a single data point close to the surface with near 0 measured radiometry on all 4 channels, we recommend to mark it as “4”.

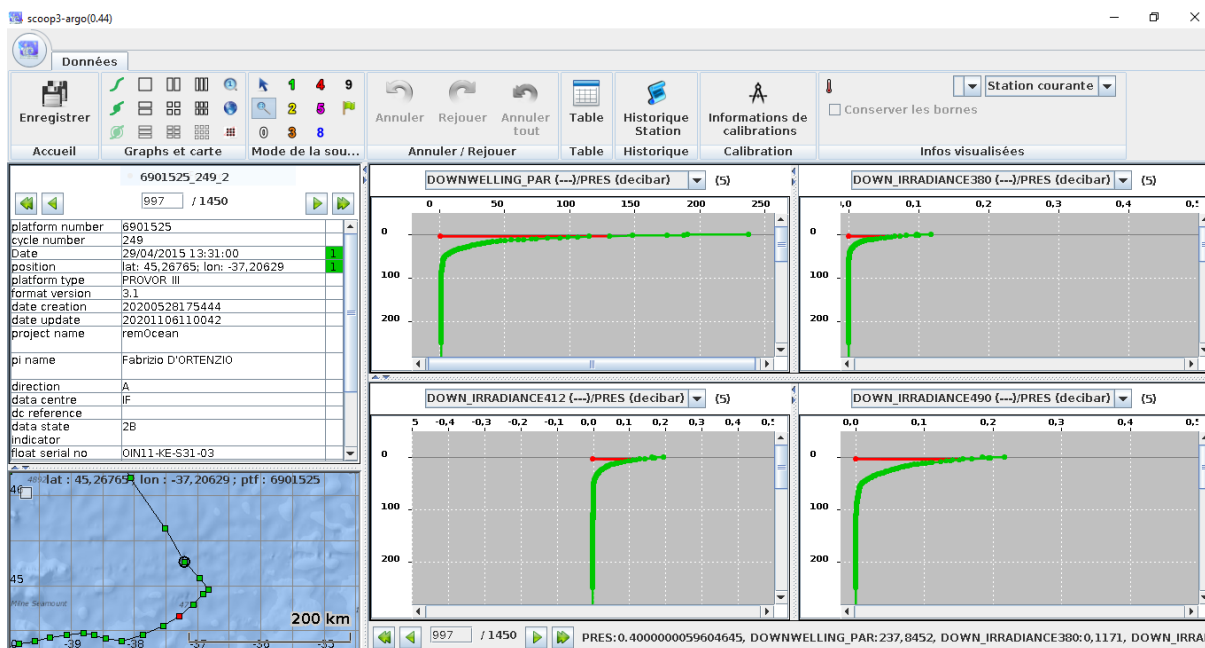


Figure 17: Screenshot of the visual QC in progress in Scoop-Argo on a profile featuring a common issue.

3.1.4 RADM operations

The software we developed in the framework of Euro-Argo RISE is named RADM (for RAdiometry Delayed Moden, available at https://github.com/qjutard/radiometry_QC). It can be obtained by downloading the latest numbered version as an archive or by cloning the repository. At the time of writing, the current version is 1.03, which has been used to realize the DM operations for most of the floats we considered. A short tutorial for the DM operator on how to install and use RADM is provided in the appendix.

3.2 Process to correct past data

For past data and for floats that may not have good ancillary data available, we recommend to follow the same general process but with the option to use the alternative methods described in section 2.2.2.3.

In practice the general process shown on figure 16 is the same with the addition that the operator should consider both the main and alternative methods together when judging the adequacy of the aging/temperature correction (steps 3 and 8 on figure 16). This possibility is currently offered by default in RADM (1.03) which always shows the results of the alternative methods. The operator can then decide between main and alternative methods (or neither), details can be found in the appendix.

3.3 Additional information in DM files

In this section we explain the choices we made regarding the additional data that is filled in corrected NetCDF files. These additional fields are all automatically filled in RADM when writing DM files.

3.3.1 QC flags

The DM-QC flags on sensor aging and temperature corrected profiles are assigned to the <PARAMETER>_ADJUSTED_QC axis according to the following procedure:

1. Recover the QC flags assigned with the visual QC (<PARAMETER>_QC). These profiles may contain Flags “1”, “2”, “3” and “4”;
2. Detect the dark values within corrected profiles by applying successive Lilliefors tests (following Organelli et al. 2016), and assign Flag “2”;
3. Change radiometry flags that were set to “3” or “4” after visual QC to “4”;
4. If the pressure QC flag is “3” or “4”, the radiometry flag is assigned as “4”;
5. If T_s cannot be reconstructed, the radiometry flag is assigned as “4”.

It may seem counterintuitive in step 2 that we change the flags in the dark part of profiles to “2” when the real-time adjusted flag is “1”, effectively degrading the quality of the profiles in the specific section for which we provide an improvement. This is because we have greater expectations for the quality of the data in DM than in real-time. The dark part of profiles was mostly considered “good” (“1”) in RTQC but we consider it as only “probably good” in DMQC, even after correction.

In step 3 we change flags “3” to “4” in DMQC, this is a choice to not include “probably bad” data (flag “3”) in Delayed Mode and instead classify them as “bad” (flag “4”) with a corresponding fill value in the <PARAMETER>_ADJUSTED axis.

3.3.2 Errors

In the <PARAMETER>_ADJUSTED_ERROR field we provide an error estimation of the corrected data. This error estimation does not correspond to a propagation of uncertainties and instead represents the remaining noise in the data. For each parameter, we expressed it as the maximum between a constant noise equivalent irradiance (NEI) and a relative error (ER) that is proportional to the corrected value of the parameter (<PARAMETER>_ADJUSTED):

$$\sigma_{E_d} = \max(NEI_{E_d}; ER_{E_d} \cdot E_{d_{corrected}})$$

NEI_{E_d} is the manufacturer’s NEI value of OCR-504 radiometers equal to $2.5 \cdot 10^{-5} \text{ W m}^{-2} \text{ nm}^{-1}$ for all $E_d(\lambda)$ [9]. For PAR, NEI_{E_d} was estimated by computing the maximum standard deviation observed for the dark values at the 1000 dbar parking depth corrected for any aging among a total of 34 selected floats. The resulting NEI_{E_d} for PAR is equal to $0.03 \mu\text{molQuanta m}^{-2} \text{ s}^{-1}$. ER_{E_d} is 5% for PAR [5] and 2% for $E_d(\lambda)$ following previous calibration error estimations [3][10].

The resulting error estimation is illustrated on figure 12 as a grey error ribbon around the corrected data.

3.3.3 Metadata

In RADM version 1.03, the Argo metadata written in NetCDF Delayed Mode files is as follows:

- **SCIENTIFIC_CALIB_COMMENT** = “<PARAMETER> dark correction. Uses JULD to correct drift and SENSOR_TEMP to correct temperature variance. SENSOR_TEMP is reconstructed from the TEMP axis of the core file following [<https://doi.org/10.13155/62466>]”

The DOI refers to the documentation on radiometry QC [8] which will be updated to include the delayed mode documentation.

- **SCIENTIFIC_CALIB_EQUATION** = “<PARAMETER>_ADJUSTED = <PARAMETER> - A - B*SENSOR_TEMP - C*JULD”
- **SCIENTIFIC_CALIB_COEFFICIENT** = “A = <VALUE>, B = <VALUE>, C = <VALUE>, Q = <VALUE>”
 <VALUE> is always expressed with 4 significant numbers. The value of Q is only written if Q is not 0, that is if a quadratic regression has been used in the aging correction for this particular parameter.
- **HISTORY_SOFTWARE** = “RADM”
- **HISTORY_SOFTWARE_RELEASE** = “1.03”

4 Database improvements and conclusion

The improvement of the database by the DM process has already been covered in the R&D section of the DM because the dataset tested was extensive (see section 2.2.3). All no longer profiling coriolis floats (131 floats) were considered combining 24217 profiles. A DM correction could be provided for 76% of the considered profiles (18312 corrected profiles) in late 2020 and early 2021 (figure 18). At the time of writing, around half of all radiometric profiles available in the coriolis DAC have a delayed mode correction available.

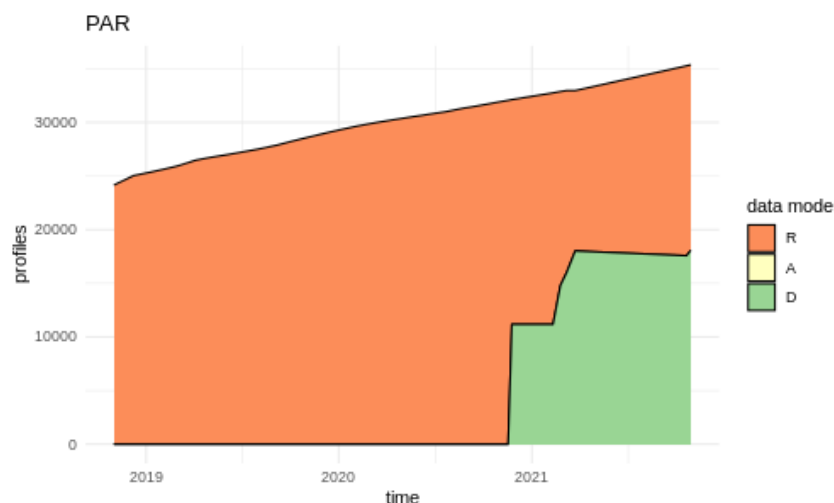


Figure 18: Evolution of the data mode status of radiometric profiles in the coriolis DAC.

The DM process for irradiance data has been clearly defined and is focused on potential issues with the dark values. A tool (RADM) was developed to assist the DM operators in their work. The entire

DM process (including visual QC) can be completed in less than an hour by a trained operator. This is compatible with the objective to realize the DM for a global fleet of 1000 BGC floats every 6 months to a year, provided that the necessary workforce is put in place (equivalent to 6 to 12 man months per year).

Appendix: RADM tutorial

Installation

The Radiometry Delayed Mode (RADM) software is not standalone and is only presented as a codebase, mostly written in R. All of what is described here refers to version 1.03, which was used to realize the DM-QC of most floats at the time of writing. In order to use RADM you will need to use a UNIX operating system and to have installed R and the necessary libraries, which are listed in “start_RADM.R”. The local paths should be updated in “pathways.R” and “RADM.sh”. Note that, as of version 1.03, the software expects the folder tree to follow ftp.ifremer.fr ; The NetCDF files for float <WMO> should be in “path_to_netcdf/<WMO>/profiles/”. RADM also expects to find a folder at “path_to_netcdf/<WMO>/profiles/RADM/RADM_profiles” in order to write the corrected NetCDF files. A version of “argo_bio-profile_index.txt” is included but the latest version can be downloaded from <ftp://ftp.ifremer.fr/ifremer/argo/>. These requirements are rather rigid and we are looking into streamlining them for future versions.

Usage

The software can be launched by launching RADM.sh from anywhere, we recommend assigning an alias named “RADM” to the RADM.sh file location. When the alias is set “RADM -h” shows the software options, the DM on float <WMO> can be initiated with the command “RADM -W <WMO>”.

RADM is text based and presents the operator with numbered menus that they can make decisions from. The plots on the basis of which the operator makes decisions (figures 9, 10, and 11) are presented in separate windows. On figure 19 and 20 (split in 2) we show the full RADM process on float 6901584, in the following we will go through the steps that were taken to correct this float.

The operator must first specify the sensor that the float is equipped with, this is necessary to use appropriate parameters when reconstructing the sensor’s temperature.

Then the operator is presented with figures similar to 9 and 10, along with corresponding figures for the alternative method (method B, the alternative methods can be ignored for future deployments with good ancillary data). They then find that the linear fit is not adequate for $E_d(412)$ and select option 3 to change to a quadratic fit, they select a quadratic fit only for $E_d(412)$. RADM presents the operator with figure 9 and 10 (and corresponding method B figures) and they decide to continue with the main method (method A).

RADM computes both temperature effects correction methods and presents figure 11 and the corresponding alternative method (which can be ignored for future deployments with good ancillary data), the operator is satisfied with the result of the main method and validates the correction.

RADM then checks whether any date information is missing (or flagged as bad) in profiles, in such a case it would provide the operator with options to compute the aging correction on these profiles. This option does not fill the missing date information. RADM also checks for any missing (or flagged as bad) position information and informs the operator of the affected profile(s). This does not affect the computation of the DM corrected NetCDF files.


```
Importing libraries and source code...DONE
Importing bio index and greylist...DONE
What kind of radiometry sensor is used in this float ? (0 to abandon and quit)

1: OCR504 (PEEK)
2: OCR504 (Aluminium)

Selection: 1
Preparing file lists, dates, and greylist...DONE
Importing and extracting drift data...DONE
Extracting dark data for method B...DONE
Flagging outliers and greylist...DONE
Fitting both methods...DONE
Creating drift plots...DONE
What is the next step ? (0 to abandon and quit)

1: Continue with correction from method A
2: Continue with correction from method B
3: Change to quadratic fits for some parameters
4: Continue without a drift correction

Selection: 3
Use a quadratic fit for DOWNWELLING_PAR ?

1: Yes
2: No

Selection: 2
Use a quadratic fit for DOWN_IRRADIANCE380 ?

1: Yes
2: No

Selection: 2
```

Figure 19: Screenshot of the full RADM operations for the DM of float 6901584 (first part).

```
Use a quadratic fit for DOWN_IRRADIANCE412 ?
1: Yes
2: No

Selection: 1
Use a quadratic fit for DOWN_IRRADIANCE490 ?
1: Yes
2: No

Selection: 2
Fitting both methods...DONE
Creating drift plots...DONE
What is the next step ? (0 to abandon and quit)
1: Continue with correction from method A
2: Continue with correction from method B
3: Change to quadratic fits for some parameters
4: Continue without a drift correction

Selection: 1
Extracting day and night profiles...DONE
Flagging greylisted profiles and outliers in day profiles...DONE
Extracting full Ts range...DONE
Fitting Ts to radiometry parameters...DONE
Creating Ts/Irr plots...DONE
Which correction should be used ? (0 to abandon and quit)
1: Continue with correction from night method
2: Continue with correction from day method
3: Add or change the pressure cutoff for data selection

Selection: 1
No profiles with missing date
No profiles with missing position
Applying correction to netcdf files...
```

Figure 20: Screenshot of the full RADM operations for the DM of float 6901584 (second part).

References

- [1] Jerome Detoc, Mickael Garo, Thierry Carval, Baptiste Thepault, and Pierre Mahoudo. Scoop-argo : visual quality control for argo netcdf data files. SEANOE, <https://doi.org/10.17882/48531>, 2017.
- [2] Watson W Gregg and Kendall L Carder. A simple spectral solar irradiance model for cloudless maritime atmospheres. *Limnology and oceanography*, 35(8):1657–1675, 1990.
- [3] Stanford B Hooker, Elaine R Firestone, Scott McLean, Jennifer Sherman, Mark Small, Gordana Lazin, Giuseppe Zibordi, James W Brown, and Charles R McClain. The seventh seawifs intercalibration round-robin experiment (sirrex-7), march 1999. Technical report, 2002.
- [4] Quentin Jutard, Emanuele Organelli, Nathan Briggs, Xiaogang Xing, Catherine Schmechtig, Emmanuel Boss, Antoine Poteau, Edouard Leymarie, Marin Cornec, Fabrizio D’Ortenzio, et al. Correction of biogeochemical-argo radiometry for sensor temperature-dependence and drift: Protocols for a delayed-mode quality control. *Sensors*, 21(18):6217, 2021.
- [5] Matti Möttöus, Madis Sulev, Frédéric Baret, Raoul Lopez-Lozano, and Anu Reinart. Photosynthetically active radiation: measurement and modeling. In *Encyclopedia of sustainability science and technology*, pages 7970–8000. Springer, 2012.
- [6] Emanuele Organelli, Hervé Claustre, Annick Bricaud, Marie Barbieux, Julia Uitz, Fabrizio d’Ortenzio, and Giorgio Dall’Olmo. Bio-optical anomalies in the world’s oceans: An investigation on the diffuse attenuation coefficients for downward irradiance derived from biogeochemical argo float measurements. *Journal of Geophysical Research: Oceans*, 122(5):3543–3564, 2017.
- [7] Emanuele Organelli, Hervé Claustre, Annick Bricaud, Catherine Schmechtig, Antoine Poteau, Xiaogang Xing, Louis Prieur, Fabrizio D’ortenzio, Giorgio Dall’Olmo, and Vincenzo Vellucci. A novel near-real-time quality-control procedure for radiometric profiles measured by bio-argo floats: Protocols and performances. *Journal of Atmospheric and Oceanic Technology*, 33(5):937–951, 2016.
- [8] Antoine Poteau, Emanuele Organelli, Emmanuel Boss, and Xiaogang Xing. Quality control for biogeochemical argo radiometry. <https://doi.org/10.13155/62466>, 2019.
- [9] SATLANTIC, Satlantic LP: Halifax, NS, Canada. *Operation Manual for the OCR-504*, 2013.
- [10] Kenneth J Voss, Scott McLean, Marlon Lewis, Carol Johnson, Stephanie Flora, Michael Feinholz, Mark Yarbrough, Charles Trees, Mike Twardowski, and Dennis Clark. An example crossover experiment for testing new vicarious calibration techniques for satellite ocean color radiometry. *Journal of Atmospheric and Oceanic Technology*, 27(10):1747–1759, 2010.